International Journal of Science and Research (IJSR)
ISSN (Online): 2319-7064
Index Copernicus Value (2016): 79.57 | Impact Factor (2015): 6.391

Parameters Affect the Efficiency of Acousto-Optic Modulators

Suha Mousa Alawsi[1], Lubaba abdul Kareem Al- Janabi[2]

[1]Al-Nahrain University- College of Science- Dept. of Physics
suhaalawsi[at]gmail.com
[2]Al-Nahrain University- College of Science- Dept. of Physics
lubabaaljanabi[at]yahoo.com

Abstract: ***In this paper, an acousto optic modulator (AOM) is designed, in which four materials are tried to be used in the head of the modulator; LiNbO3, TeO2, Ge, and SiO2. The efficiency of the modulation is considered with respect to the use of each material at four considered frequencies; 200, 300, 400, and 500 kHz. Three considered diffraction efficiency measures are computed using MatLab programming language, they are: acoustic power, Bragg angle, and Q-factor. Then, the results are analyzed to decide the best design and situations that give best modulation results. The diffraction efficiency is directly proportional to the acoustic power when the operating parameters are set to suitable values. It is found that the $LibNO_3$ based AOM has been presented higher diffraction efficiency than other materials. In such case, $LiNbO_3$ is the best used material that showed less Brag angle and then higher efficiency relative to other used materials. Also, only $LiNbO_3$ material is operated in Raman-Nath regime at the frequency 200 kHz, while it is operated in Bragg diffraction regime at other considered frequencies. The highest modulator efficiency of the designed acoustic modulator was about 95% using $LiNbO_3$ material.***

Keywords: Acousto-optic modulator, transmission of AO modulator, Bragg angle diffraction, crystal material of AOM, diffraction efficiency of AOM, Q-factor

1. Introduction

The field of acousto-optics is describing the effect of light-sound interaction, which occurs due to the fact that a sound wave induces localized refractive index variations in the medium through which it travels. This interaction is not just a curiosity but form the basis of a whole range of practical devices. Moreover, the effect is relatively strong, and important parameters such as amount of light deflected, angle of deflection, and frequency shift are directly related to sound power and sound frequency; which can be controlled electronically. **Such interaction** can be thought as a mixing process that resulting sum or difference frequency generation between phonons and photons. Figure (1) shows a simple setup of AO experiment, it consists of a water-filled glass tank into which a sound wave frequency fs is launched by means of a transducer **[1].**

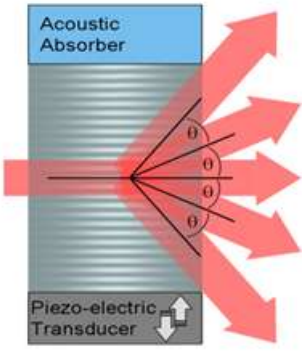

Figure1: Experimental setup of AO [1]

The far end of the tank is lined with a sound absorbing material in order to prevent reflections. When a collimated beam of light is made to impinge on the tank from the left, it observed that the light leaving the tank is split into many orders, labeled -2, -1, 0, +1, +2, etc., in the drawing. Upon increasing the sound power the number of orders visible is seen to increase gradually, although any one of the appears to go through maxima and minima for specific sound levels. The angle between the various orders does not depend on the sound amplitude. If one change the sound frequency, the deflection angles change, and careful measurement reveals that the nth order is characterized by an angle È, where ë and Ë denoting the wavelengths of light and sound, respectively It thus appears that the sound wave acts like a thin phase grating with a grating period equal to the sound wavelength and a refractive index variation [2]. The rarefactions and compressions in the sound wave induce a periodic change in the refractive index of the medium. The fact of moving the sound wave (and hence the induced grating) upward with sound velocity (Vs) give a Doppler shift which is given by the following formula for the nth order:

Ä/ =f\(Vs sin n)/c = nfs … (1)

Where f and c denote the frequency and velocity of the light. Frequency measurements on the various orders do, in fact, indicate that the nth order is upshifted (or downshifted when n is negative) by n times the frequency of the sound If a standing wave is used in the experiment, each of the orders will be observed to be modulated, rather than frequency shifted, at a frequency fs. The sound wave may now be thought of as inducing a stationary grating with a. The simple experiment described above has revealed some very interesting phenomena which may well be put to use in a practical device: modulation, deflection, and frequency shifting. The engineering aspects of acousto-optics are essentially concerned with optimizing these effects for specific applications [3].

2. Related Work and Contribution

The problem of AO modulator design has attracted a lot of researches. The application field was still searching to an accurate design that can be used to improve the modulation results. The most interesting researches besides our contribution are briefly explained in the following subsections:

2.1 Related Work

There are many papers devoted to AO modulator simulation and design. They differ in many aspects such as; shape, used materials, power supply, wavelength, or even the application limitations. The feasibility of using the high speed characteristic to design effective modulators is investigated in [4], in which the problem of the strong acousto-optic interaction is analytically solved in three dimensional computation, the results are compared to two numerical algorithms of different split-step. The first algorithm depends on the concept of Fourier-optics, whereas the second relies on more rigorous wave equation approach. In [5], a newly simple cascaded acousto-optic system to perform image processing is presented. The system composed of two imaging lenses and two acousto-optic modulators are put in sequenced form. Computer simulation is given and compared to an optical image processing system which uses a single acousto-optic modulator. While [6] studied a computer simulation by using MATLAB software to deduce the value of design parameters such as Klein-Cook Q- parameter and crystal efficiency at the acoustic frequencies. Experimental work involves two parts: optical and electrical. The optical part used Lithium Niobate ($LiNbO_3$) crystal as nonlinear crystal and He-Ne laser of 632.8 nm wavelength and 1 mw output power. While the electrical part which is constructs the trigger circuit and high voltage. Also, [7] presented a numerical simulation of acousto-optic tunable filters based on multi- reflection beam. Planer waveguide filters based on the thin film of $LiNbO_3$ by using FDTD method. The results showed that the AO filters have very good dispersion properties and extremely small size provide a narrow filtration line. In [8], the interaction between Bragg gratings and acoustic waves is investigated by numerical method for suspended core fibers. It is found that the side lobe is reflectivity increasing by 28% in comparison with standard fibers. This result indicates the possible achievement of efficient optical modulators. In [9], the method for analyzing the anisotropy of acousto-optic figure of merit is presented in terms of optically uniaxial crystals. This article deals with analysis of the isotropic acousto-optic interaction. The results of the calculations agree well with the experimental data known from the literature. Whereas, [10] presents a search method for matching Bragg acousto-optic geometries, which is providing a largest acousto-optic figure of merit M_2 for diffractions of isotropic and anisotropic. The result of applying such method on $LiNbO_3$ showed the maximum acousto-optic figure of merit is $10.88X10^{15}$ (S^3/kg).

2.2 Contribution

The present work aims at analytical studying the requirements of acousto optic modulator design. The analysis leads to determine the characteristics of the designed modulator and then use the simulation technique to implement the proposed design and improve the performance efficiency by employing the determined modulator characteristics. The simulation enables to operate the designed AO in different situations with the variation of some determined parameters. Also, four different types of materials are employed in the frequent practices to estimate the acousto-optic properties that may affect the performance efficiency of the proposed AO design.

3. Proposed AOM Design

The proposed AOM design is carried out by Comsol software, which is commonly used to design and simulate acousto optic modulators. The available tools in this software enable to introduce the best boundary conditions that suitable in use with the material of proposed modulator establishment. The designed model of acousto-optic modulator is shown in Figure (2), it consists of acousto-optic medium of dimensions 3×4 cm and 3×0.5 cm respectively. The piezoelectric transducer is created with dimension (0), the piezoelectric domain is chosen from PZT-5H material (Lead Zirconate Titanate) that is a commonly used material in piezoelectric transducers, while the optic crystal domain is considered in three cases according to the used material: the first is the use of Lithium Niobate (LiNbO3), the second is the use of fused silica (SiO_3), while the third is the use of Germanium (Ge), and the fourth one is the use of Tellurium dioxide (TeO_2). This model simulates a single crystal plate in such a structure. The element is rotationally symmetric, making it possible to set up the model as a 2D axially symmetric problem.

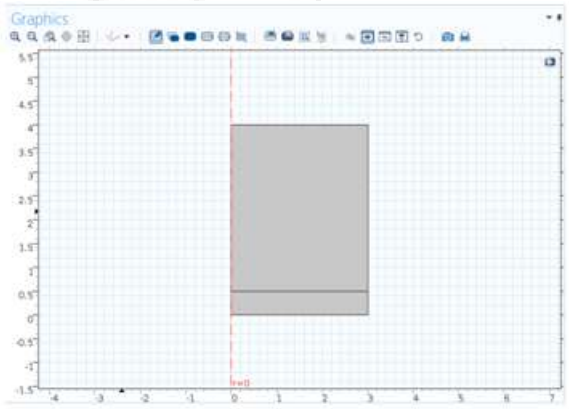

Figure 2: Geometry of proposed acousto-optic modulator design

The piezoelectric material is modeled by solving the Solid Mechanics and Electrostatics physics that are coupled via the linear constitutive equations that correlate stresses and strains to electric displacement and electric field. These physics interfaces solve for the balance of body forces and volume charge density respectively as $\nabla.\sigma = 0$ and $\nabla.D$=0. This coupling is automatically implemented in COMSOL Multi-physics by the Piezoelectric Effect node located under the Multi-physics branch in the Model Builder. The settings of the boundary conditions for the modulator model that initially build are leads to determine the characteristics of the designed modulator. Table (1) presents the operating parameters of the proposed AO modulator. These parameters

are input to Comsol at the model building stage. The values of these parameters are optimized by trial and error to achieve the optimal value of each parameters that given in the table. The first three parameters are related to the modulator size, then the input power is determined as the fourth parameter, the fifth parameter determine the location of interaction in the designed modulator, then the wavelength of the used light is determined as sixth parameter, the seventh and eighth parameters are related to the room temperature that determine the temperature of the modulator environment.

Table 1: Operating parameters of proposed AOM for different materials

Operating Parameters		Value and Unit
Interaction length (L)		L = 3 cm
Modulator height (H)		H = 4 cm
Laser beam diameter (D)		D = 1 mm
Acoustic power (P_a)		0.5 watt $\leq P_a \leq$ 2.5 watt
Focal length (F)		F = 3mm
Operating signal laser wave length (λ)		λ = 1.6 μm
Room temperature (T_0)		T_0 = 300 K
Ambient temperature (T)		300 K $\leq T \leq$ 340 K
$LiNbO_3$ Lithium niobate Based AOM device	Material density	ρ = 4644
	Refractive index	n = 2.2
	Acoustic velocity	$V_a = 6.6 * 10^3$ m/sec
	Figure of merit	$M_2 = 7$ cm^2/sec
	Attenuation	α = 0.15 dB/$GH_{Z.cm}$
SiO_2 Fused silica Based AOM device	Material density	ρ = 5606
	Refractive index	n = 1.46
	Acoustic velocity	$V_a = 5.96 * 10^3$ m/sec
	Figure of merit	$M_2 = 1.5$ cm^2/sec
	Attenuation	α = 6.45 dB/$GH_{Z.cm}$
TeO_2 Tellurium dioxide Based AOM device	Material density	ρ = 4260
	Refractive index	n = 2.25
	Acoustic velocity	$V_a = 4.26 * 10^3$
	Figure of merit	M_2 = 34
	Attenuation	α = 4.75 dB/$GH_{Z.cm}$
Ge Germanium Based AOM device	Material density	ρ = 5323 kg/m^3
	Refractive index	n = 4
	Acoustic velocity	$V_a = 5.5 * 10^3$
	Figure of merit	M_2 = 180
	Attenuation	α = 10.5 dB/$GH_{Z.cm}$

Due to it is intended to use different crystal material, there are five operating parameters are determined of each material, the first is the material density, the second is the refractive index of the material, the third is the acoustic velocity that measured according to equation $V_a = d / t$ Where, d represents the diameters of the optical beam waist. Higher modulator speed is obtained when t is as small as possible, that indicates the modulation speed, the fourth one is the figure of Merit, while the fifth is the attenuation. Except the acoustic velocity, the remaining four parameters are constants for each material, while the acoustic velocity is varying according to the rise time and beam diameter.

4. Efficiency of AOM

There are many parameters can be regarded to find the efficiency with boundary condition for solving the equations of parameters that affect the diffracted efficiency (DE) of AO modulator. Terminology, DE is indicating the ratio between the output zero-ordered intensity I_{0th} and first-ordered intensity I_{1st} beam that calculated by equation (2).

$$DE = I_{1st}/I_{0th} \quad (2)$$

In addition, the device undergoes the insertion losses (IL) due to absorption in the bulk material, the losses in A/R coated surface can be represented in equation (3)

$$IL = 1 - I_{0th}/I_{laser} \quad (3)$$

So the total efficiency E_t is given in equation (4).

E_t=DE x (1-IL) % (4)

MatLab is used to programming the mathematical relations that related to the efficiency. The following subsections indicate the procedure of estimating the performance efficiency:

4.1 Acoustic Power

Maximum diffraction efficiency is achieved at optimum acoustic or RF drive power that given by equation (5). Accordingly, the RF drive power is related to the squared wavelength λ, whereas the efficiency of the first-ordered diffraction is related to the RF drive power according to a squared sine function. Implies, the relative efficiency (ε) is determined by the formula ($\varepsilon = sin^2 \pi/2.\sqrt{p_{in}}/\sqrt{p_{sat}}$) when the device operate at power (P) is less than the P_{sat}. Thus, the RF driver is switched in between the zero and P_{sat} in digital (On: Off) modulation form. Also, the RF driver can be proportionally controlled in analog modulation using the first-ordered intensity.

$$P_{sat} = \frac{k\lambda^2 H}{2LM_2} \quad (5)$$

where, L is the length of interaction (electrode), λ is the wavelength, H is the height of electrode, M_2 is figure of Merit, k is the loss of transducer conversion.

4.2 Bragg angle

The Bragg angle is computed by equation(6), in which the acoustic frequency (f) is predefined by setting the acoustic set, whilst the acoust is stipulated in the device datasheet, and t is the transit time that estimated throughout the operating mode.

$$\theta_{Bragg} = \frac{\lambda f}{2V} \quad (6)$$

Where, λ is the wavelength, f is RF frequency, and V is acoustic velocity.

4.3 Q-Factor

The modulation frequency and optical power density that satisfying the Bragg criteria in the AO design are important parameters to measure the performance efficiency of the modulator. The Bragg condition is measured by the Q-factor according to equation (7). The value of Q should be less than 10 for strong Bragg diffraction. The device appears some sensitivity to angular alignment and intolerant of input beam divergence (or convergence) when the Q-factor is very high. But when the value of Q-factor is less than 5, then a significant percent of zero-ordered beam that diffracted into higher-orders (Output beams at multiple angles) is noticed. Also, equation (7) is easily programmed to compute the performance efficiency that related to the Q-factor.

$$Q = 2.\pi.(\lambda.L.f^2 / n\,.\,V^2) \quad (7)$$

5. Results and Discussions

Figure (3) shows the relational behavior of the diffraction efficiency versus the acoustic power for the four considered materials: LiNbO3, TeO2, Ge, and SiO2. It is shown that the diffraction efficiency is directly proportional to the acoustic power when the operating parameters are set to suitable values. The diffraction efficiency is related to the figure of merit of the used material, which directly affect the diffraction efficiency. It is shown that the $LibNO_3$ based AOM has been presented higher diffraction efficiency than Ge material, Ge material gives higher efficiency than SiO_2 material, and then SiO_2 material gives higher efficiency than TeO_2 material. The efficiency differences between them are expanded with increasing the acoustic power. The monotonic linear behavior of the efficiency can be predicted the efficiency value that out of the used range.

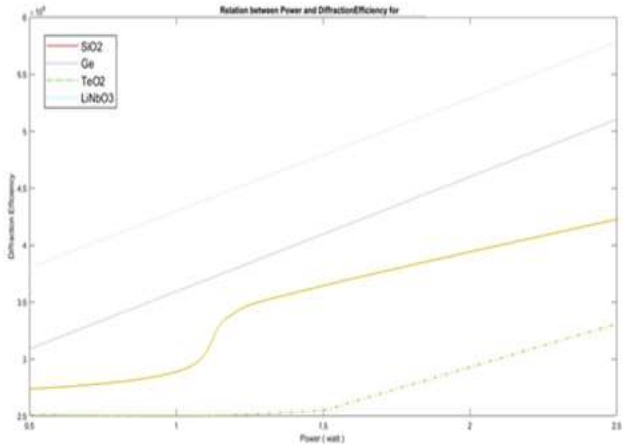

Figure 3: Relational behavior of the diffraction efficiency versus power

Figure (4) shows the relational behavior of normalized diffraction efficiency as a function of Brag angle for the four considered materials: LiNbO3, TeO2, Ge, and SiO2. It is shown that the diffraction efficiency is normally distributed as a bell shape with the variation of Brag angle when the operating parameters are set to suitable values. Due to the use of symmetric extended scale of Brag angle from the negative to positive values, the distribution of the diffracted efficiency is shown symmetric about the vertical axis. It is noticeable that the Bragg angle will reduce the efficiency, and optimum efficiency is achieved when the incident light is input to the AOM at zero Bragg angle. Bragg angle errors will reduce efficiency the diffraction efficiency is also related to Brag angle, the variation of Brag angle governs the efficiency values, in which the efficiency decreases with increasing the Brag angle from the zero value. The width variation of the efficiency behaviors are related to the optical features of the used materials, the best efficiency is decided for the least width of efficiency distribution. In such case, LiNbO3 showed the best efficiency in terms of Brag angle, this behavior indicates the sensitivity and the response of the AOM.

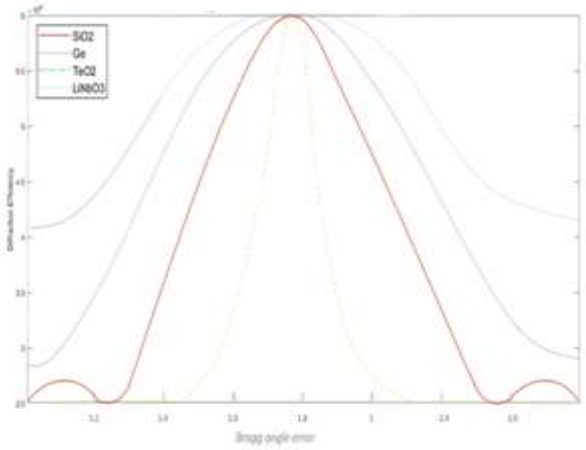

Figure 4: Relational behavior of the diffraction efficiency versus Bragg angle error

Figure (5) shows the relational behavior of Brag angle based diffraction orders as a function of frequency for the four considered materials: LiNbO3, TeO2, Ge, and SiO2. It is shown that the Brag angle is linearly related to the frequency with a direct proportional relationship. It should be mentioned that the negative values of the Brag angle do not appear in this figure due to the Brag angle is a positive pointer of diffraction amount and the negative sign, if found, refers to the opposite direction only. Such behaviors indicate that greater efficiency may be achieved at less Brag angles that corresponding to fewer frequencies. In such case, $LiNbO_3$ is the best used material that showed less Brag angle and then higher efficiency relative to other used materials. The differences between the Brag angle values for the four considered materials are increasing with increasing the frequency leading to decrease the diffraction efficiency. Also, the monotonic behavior of the Brag angle as a function of frequency can be predicted for other values that out of the used range.

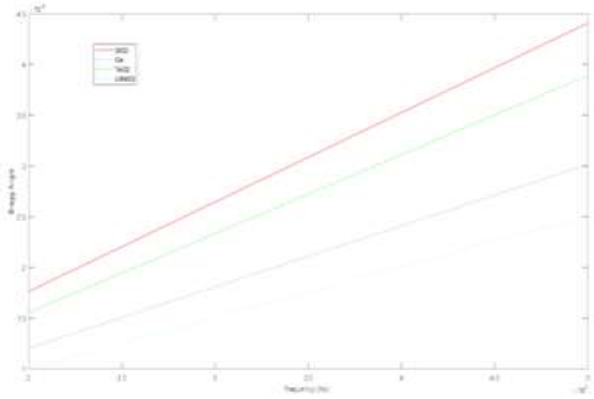

Figure 5: Relational behavior of the Brag angle versus frequency.

Table (2) presents the resulted Q-facor values for the four considered materials : $LiNbO_3$, TeO_2, Ge, and SiO_2, while Figure (6) pictures the Q-factor values listed in Table (2). It is shown that the Q-facor increases with increasing the frequency. The increase impact the Q-factor behavior relative to others that belong to other materials are gradually increased with the frequenct.

Table 2: Resulted Q-factor for the four considered materials

f(kHz)	Q-factor			
	$LibN0_3$	Ge	SiO_2	$Te0_2$
200	0.5	0.9	1.8	2.76
300	0.9	2.1	4.02	6.21
400	1.16	3.74	7.2	11.04
500	1.45	5.84	11.25	17.25

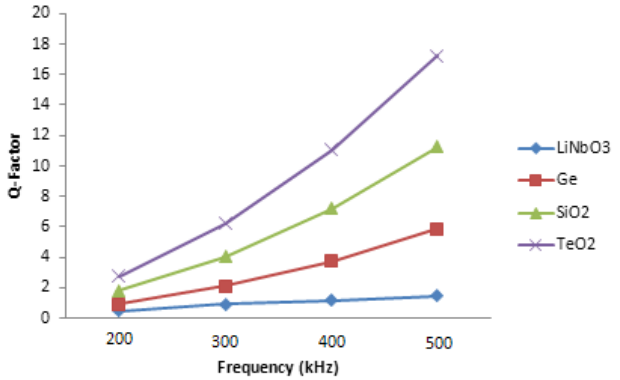

Figure 6: Q-factor behaviors versus frequency

Due to the Q-factor is regarded as a parameter used for examining AO interaction geometries, a large quantity of nonzero-ordered light are transmitted into diffraction region. This parameter indicates the difference in the phase of different partial waves as a result of different propagation directions. In the case when Q is less or equal to 0.6, then the AO interaction is in Raman-Nath regime that make the result of multiple orders of diffraction are same as that of thin diffraction grating. Whereas, when Q-factor is greater or equal to 0.8, then the acoustic grating is no longer thin and operating in Bragg diffraction regime. In such case, the AO interaction will be more sensitive to the incidence angles of the beam, which is useful in experimental work because of the transferred energy becomes very significant between light waves of the same phase and the diffracted light, which is predominantly single-ordered appearing.

Therefore, it is shown in figure (6) that only $LiNbO_3$ material is operated in Raman-Nath regime at the frequency 200kHz, it is operated in Bragg diffraction regime at frequencies else that. Whereas, other three considered materials are all operated in the Bragg diffraction regime. This ensures that the use of $LiNbO_3$ material showed the best performance efficiency in comparison with other considered materials.

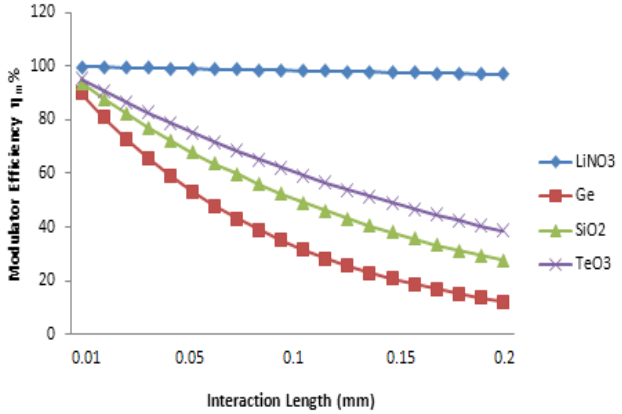

Figure7: Modulation efficiency behaviors versus interaction length

The modulator efficiency η_m dependent on the length of interaction in acoustic modulator and attenuation of materials, in figure (7) show that the modulator efficiency of acoustic modulator made from $LiNbO_3$ material is more than the other materials because the attenuation coefficient is α = 0.15 dB/GH_z .cm less than other materials, but generally the efficiency of modulator decreases with increases the interaction length.

6. Conclusions

1- It is shown that the $LibNO_3$ based AOM has been presented higher diffraction efficiency than Ge material, Ge material gives higher efficiency than SiO_2 material, and then SiO_2 material gives higher efficiency than TeO_2 material.

2- The efficiency decreases with increasing the Brag angle from the zero value In such case, LiNbO3 showed the best efficiency in terms of Brag angle, this behavior indicates the sensitivity and the response of the AOM.

3- Only $LiNbO_3$ material is operated in Raman-Nath regime at the frequency 200 kHz, it is operated in Bragg diffraction regime at frequencies else that.

4- The modulator efficiency of acoustic modulator made from $LiNbO_3$ material is more than the other materials because the attenuation coefficient is α = 0.15 dB/GH_z .cm less than other materials, but generally the efficiency of modulator decreases with increases the interaction length.

References

[1] B. E. A. Saleh and M. C. Teich, Fundamentals of Photonics, 2nd ed.: Wiley, 2013.

[2] Chien Aun Chan, “Remote Repeater-Based EPON with MAC Forwarding for Long-Reach and High Split Ratio Passive Optical Networks,” J. Opt. Commn. Network, Vol. 2, No.1, pp.28-37, 2011.
[3] S. Chase. "Fabrication of Binary Phase Diffusers for Space Variant Processing”,M.S. Thesis, Dept. of Electrical Engineering, Texas Tech University, Dec. 2002.
[4] Y. Young and E. Yao, “Design Consideration for Acousto-Optic Devices,” Proceedings of IEEE, Vol. 69, No. 1, pp. 54-64, 2005.
[5] O. S. America, Handbook of Optics: Mc Graw-Hill, 2000.
[6] A. P.Goutzoulis and D. R.Pape, Design and Fabrication of Acousto-Optic Devices: Taylor & Francis, 1994.
[7] J. Xu and R. Stroud, Acousto-optic devices: principles, design, and applications: Wiley, 1992.
[8] S. Sharangovich, "Diffraction characteristics of acousto-optic interaction in an acoustic field with a curved wave front," Russian Physics Journal, vol. 38, pp. 364-371, 1995.
[9] A. Cont and T.-C. Poon, "Simulations of bis-table acousto-optic devices using Matlab," in System Theory, 2003. Proceedings of the 35th Southeastern Symposium on, 2003, pp. 296-298.
[10] Alwan M.Alwan, D. S. Ahmed, U. N. Saleman, and I. S. Ahmed, "EFFECT OF THE PEAK PHASE DELAY ON AN ACOUSTO – OPTIC INTERACTIONS," Journal of Al-Nahrain University - Science vol. 11, pp. 89-97, 2008